Testing the use of the silica deposition fluorescent probe PDMPO to estimate in situ growth rates of diatoms

Eva Husmann, Christine Klaas ⓘ*
Alfred Wegener Institute, Helmholtz-Centre for Marine and Polar Research, Bremerhaven, Germany

Abstract

The fluorophore [2-(4-pyridyl)-5{[4-dimethylaminoethyl-aminocarbamoyl-methoxy]phenyl}oxazole], in short PDMPO, is incorporated in newly polymerized silica in diatom frustules and thereby provides a tool to estimate Si uptake, study diatom cell cycles but also determine mortality-independent abundance-based species specific-growth rates in cultures and natural assemblages. In this study, the theoretical framework and applicability of the PDMPO staining technique to estimate diatom species specific-growth rates were investigated. Three common polar diatom species, *Pseudo-nitzschia subcurvata*, *Chaetoceros simplex*, and *Thalassiosira* sp., chosen in order to cover a broad range of species specific frustule and life-cycle characteristics, were incubated over 24 h in control (no PDMPO) and with 0.125 and 0.6 μM PDMPO addition, respectively. Results indicate that specific-growth rates of the species tested were not affected in both treatments with PDMPO addition. The specific-growth rate estimates based on the PDMPO staining patterns (μ_{PDMPO}) were comparable and more robust than growth rates estimated from the changes in cell concentrations (μ_{cc}). This technique also allowed to investigate and highlight the importance of the illumination cycle (light and dark phases) on cell division in diatoms.

Diatoms are the main contributors to primary production and drivers of the biogeochemical cycles of carbon, silicon and other major elements in the world's oceans (Nelson et al. 1995; Tréguer et al. 2018). More recent studies indicate that the impact of diatoms on biogeochemical cycles is strongly dependent on species specific morphological and life-cycle characteristics (Assmy et al. 2013; Rynearson et al. 2013; Rembauville et al. 2015; Tréguer et al. 2018). Our understanding of the factors leading to diatom species specific dynamics and the resulting differential impact on vertical fluxes and transfer to higher trophic levels is however, still limited, because the impacts of environmental and biotic interactions on diatom growth could not be determined in situ. This is compounded by the fact that, in addition to environmental characteristics (i.e., temperature, light regime, nutrients) and trophic interactions, recent studies indicate that growth and division rates might be strongly influenced by intrinsic factors (physiology, internal clocks, and life cycles; Bowler et al. 2010) as well as interactions within the plankton that can affect both growth

*Correspondence: christine.klaas@awi.de

Additional Supporting Information may be found in the online version of this article.

and life cycles of phytoplankton species (Wolf et al. 2019; Pelusi et al. 2020). Because of the vast array of yet poorly known and quantifiable processes influencing species specific life cycles and mortality in natural assemblages, knowledge of species specific in situ growth rates (from which mortality can also potentially be inferred by subtracting the corresponding species specific in situ accumulation rates) can provide important cues to better understand dynamics of phytoplankton in natural systems (i.e., Behrenfeld 2010).

Shimizu et al. (2001) and Leblanc and Hutchins (2005) have pioneered the use of PDMPO [2-(4-pyridyl)-5{[4-dimethylaminoethyl-aminocarbamoyl-methoxy]phenyl}oxazole], a pH indicator and acidotropic fluorescent dye that binds to polymerizing silica and is incorporated in the silicon frustule of diatoms during cell division. Based on the above mentioned studies, PDMPO has been used to determine silicification rates in laboratory experiments and in situ (Leblanc and Hutchins 2005; Znachor and Nedoma 2008; McNair et al. 2015, 2018a,b). Because PDMPO is mainly incorporated in newly formed valves and girdle bands, it can also be used to identify newly divided cells (Fig. 1, McNair et al. 2018b).

PDMPO-derived growth rates

Since PDMPO is also a marker for newly divided cells (Fig. 1), it can be applied to investigate diatom abundance-based species specific-growth rates in cultures and more importantly, in natural assemblages (McNair et al. 2018a,b).
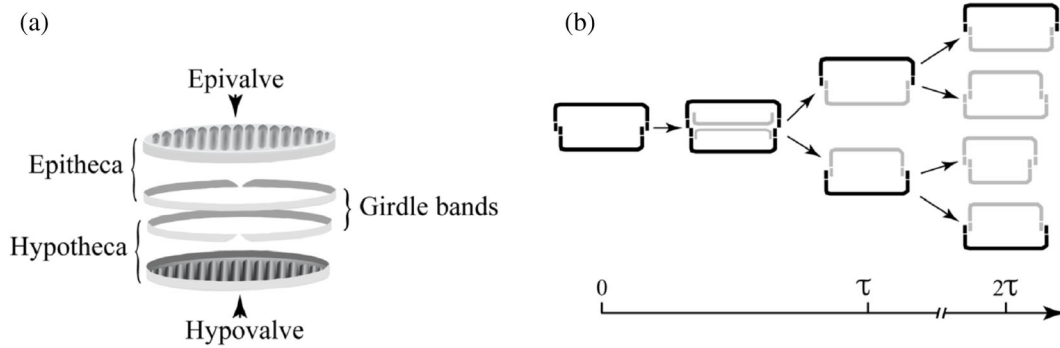
Fig. 1. Structure of the diatom frustule (**a**). Note that the hypotheca (somewhat smaller) fits in the epitheca forming a pillbox-like casing around the cell. (**b**) Cross-sectional view of a diatom frustule during mitosis. Maternal valves and girdle bands (in black) are equally divided between the two daughter cells. When PDMPO is added (here at time 0 on the horizontal scale) the dye is incorporated in the newly formed hypotheca of the daughter cells (light gray). At time τ (corresponding to 1 generation time) all cells have one half-stained frustule. Beyond one generation time, the number of half-stained cells remains unchanged (and equals 2× the number of mother cells in the population) while the number of fully stained cells increases.

Using an approach similar in concept to McNair et al. (2018*b*), and based on the following:

Provided that the population of a single species, in a natural assemblage, has uniform specific-growth rates and the population divides continuously (not synchronously) and homogenously, growth can be described as:

$$N_t = N_0 \times e^{(\mu t)} \tag{1}$$

with N_0 the number of cells at time 0, N_t the number of cells after a period of time t. The specific-growth rate μ of the population can be estimates as:

$$\mu \left[\mathrm{d}^{-1} \right] = \ln \left(\frac{N_t}{N_0} \right) \times \left(\frac{1}{t} \right). \tag{2}$$

While in culture both N_0 and N_t, and therefore μ, can be easily determined through cell counts; this is not the case for incubations with natural assemblages, where grazers and other processes lead to cell loss and consequently an underestimation of N_t. Incubations with PDMPO overcomes this issue by allowing the determination of N_0 (Eq. 2) based on the relative proportion of PDMPO stained cells (newly divided) and unstained cell at the end of an incubation as follows:

Given N_t the total cell number of a species from a subsample at a time t after PDMPO addition. $N_t = n_t + n_t'$, with n_t the total number of non-PDMPO stained cells of the species in the same subsample (cells that did not divide yet), and n_t' the total number of cells with one PDMPO stained valve (cells derived from the first division after PDMPO addition to the culture media, Fig. 1b). All things being equal (i.e., continuous and homogenous growth and loss rate for stained and unstained cells), the population (N_0) at the time when PDMPO was added that gave rise to N_t should be

$$N_0 = n_t + \left(\frac{n_t'}{2} \right) = N_t - \left(\frac{n_t'}{2} \right), \tag{3}$$

μ can therefore be estimated by inserting Eq. 3 into Eq. 2 giving:

$$\mu \left[\mathrm{d}^{-1} \right] = \ln \left(\frac{n_t + n_t'}{n_t + \frac{n_t'}{2}} \right) \times \left(\frac{1}{t} \right) = \ln \left(\frac{N_t}{N_t - \frac{n_t'}{2}} \right) \times \left(\frac{1}{t} \right). \tag{4}$$

Equation 4 is valid for conditions in which cells have divided at most only once, that is, where the incubation time does not exceed one generation time ($\leq \tau$ with $\tau = \ln(2)/\mu$). For longer incubations ($> \tau$), cells from the second generation (with both valves stained with PDMPO, Fig. 1b) should be present. Furthermore, if specific-growth rates of a species population are homogenous, no unstained cells should be present ($n_t = 0$) in incubations lasting over one generation time ($> \tau$). Given n_t'' the number of cells with both valves (fully) stained:

$$N_0 = \left(\frac{n_t'}{2} \right), \tag{5}$$

and

$$\mu \left[\mathrm{d}^{-1} \right] = \ln \left(\frac{n_t' + n_t''}{\frac{n_t'}{2}} \right) \times \left(\frac{1}{t} \right). \tag{6}$$

Generally, for incubation periods exceeding two generations (2τ), samples become dominated by fully stained cells. Specific-growth rate estimates can still be done using Eqs. 5 and 6 provided half-stained cells are abundant enough.

Hence, PDMPO staining of valves of newly divided cells allows an estimate of diatom species specific-growth or division rates in natural assemblages based on the number and proportions of nonstained, half-stained, and fully stained frustules after relatively short incubation times and without necessitating information on (1) cell concentrations at the start of the incubation, (2) the temporal evolution of cell concentrations, and (3) mortality rates.

Generally, however, the use of staining patterns (based on PDMPO or other vital stains) to estimate specific-growth rates in diatoms is based on the following assumptions: (1) Stain addition does not affect division rates. (2) Newly divided cells (daughter cells) can be readily recognized, in other words: the stain is taken up in significant quantities (i.e., visible with epifluorescence microscopy in the case of PDMPO) and only in newly formed valves. (3) Species populations do not divide synchronously. (4) The population of a single species in a natural assemblage has uniform specific-growth and mortality rates.

These assumptions, however, might not necessarily always apply, in particular when investigating natural populations in the field.

Effect of PDMPO on specific-growth rates

The impact of PDMPO on diatom specific-growth rates has been tested by Leblanc and Hutchins (2005). Their results based on incubations with natural communities suggest an optimal final concentration around 0.125 μM PDMPO and a potential impact on growth at final concentrations exceeding 0.5 μM PDMPO. Incubations with natural Antarctic diatom assemblages after addition of 0.125 μM PDMPO resulted, however, in poor signal for small weakly silicified diatoms such as *Chaetoceros debilis* (Klaas, unpubl.). Small *Chaetoceros* species are important contributors to spring blooms and carbon export in polar and temperate areas (Abelmann et al. 2006; Rynearson et al. 2013; Rembauville et al. 2015). Hence, following their growth dynamics in natural assemblages is of particular interest.

Frustule formation and PDMPO

One of the key processes in diatom life cycles is the biogenesis of the siliceous frustule. However, only a handful of observations on frustule formation during cell division in diatoms have been carried out. From the available information, silicon deposition can start with the girdle bands (during the G1 phase of the cell cycle) or with new hypovalve, depending on species (Li and Volcani 1985; Hildebrand et al. 2007, 2018; Oh et al. 2018). As long as cells with fully stained valves can be robustly estimated, the sequence in the formation of new frustules should not affect specific growth estimates with PDMPO. When using conventional epifluorescence microscopy, recognition of fully stained valves as opposed to valves where only girdle bands are stained can, however, be difficult in some species. This would be the case for species with thin valves such as needle like *Pseudo-nitzschia* and related genera.

Synchronization in diatoms

Synchronization of cell division in diatom species populations in the field has, to the best of our knowledge, never been reported and has been poorly studied. Cell division synchronization in cultured diatoms is usually only obtained through nutrient (primarily Si) and light manipulations

(Hildebrand et al. 2007). These efforts indicate that synchronization in natural environments is highly unlikely. Laboratory studies on single diatom strains have, however, shown that cell cycle and mitosis can be phased by alternating light: dark cycles (Eppley et al. 1967; Nelson and Brand 1979; Owens et al. 1980; Chisholm and Brand 1981; McDuff and Chisholm 1982), whereby mitosis might occur preferentially at night or during the daylight hours depending on species.

Depending on division rates and incubation times, synchronization and phasing of mitosis can lead to both underestimation and overestimation in specific-growth rates based on the PDMPO approach. One commonly used strategy to avoid such biases is to carry out the incubations over full (24 h) light–dark cycles.

Growth rate variability in natural species populations

To our knowledge, there are few studies specifically investigating the in situ variability in growth rates within single diatom species populations. Studies based on laboratory experiments using different strains (clones) of a species have found significant intraspecific variability in the response of phytoplankton to environmental conditions and perturbations (Brand and Guillard 1981; Brand 1989; Sjöqvist and Kremp 2016; Wolf et al. 2018). While the use of PDMPO does not allow determination of individual specific-growth rates within a species population with nonhomogenous growth, the co-occurrence of unstained cells (undivided) and fully stained valves (divided twice) are a good indicator of variability in division rates within a species population (Fig. 1). In such cases, PDMPO staining, however, can still provide a robust estimation of the whole species population specific-growth rate: in such cases, N_t the total cell number of a species in a subsample at time t after PDMPO addition is the sum of nonstained (n_t), half-stained (n_t'), and fully stained (n_t'') cells. Based on the sequence of staining during division we can estimate N_0 of the population using Eq. 3 and the population specific-growth rates using Eq. 4.

Furthermore, provided that incubation time does not exceed 2τ for the fast-growing genotypes, it is possible, based on stained cells, to give an estimate of the initial number of cells that divided twice ($n_0^{2\div}$) and once ($n_0^{1\div}$) with

$$n_0^{2\div} = \frac{n_t''}{2}, \tag{7}$$

$$n_0^{1\div} = \frac{n_t' - n_t''}{2} \tag{8}$$

and finally give an estimate of the minimum (μ_1) and maximum (μ_2) specific-growth rates of the faster growing genotypes:

$$\mu_1 = ln\left(\frac{n_t' + n_t''}{n_0^{1\div} + n_0^{2\div}}\right) \times \left(\frac{1}{t}\right), \tag{9}$$

$$\mu_2 = \ln\left(\frac{2n_t''}{n_0^{2\div}}\right) \times \left(\frac{1}{t}\right) = \ln(4) \times \left(\frac{1}{t}\right) (t < 2\tau). \qquad (10)$$

The minimum estimate (μ_1) assumes that all cells except the nonstained ones belong to this subpopulation. The maximum growth rate (μ_2) assumes that in the fast-growing subpopulation all cells have divided twice, that is the total number of cells belonging to this population at time t are all the double-stained cells plus the same amount of half-stained cells (Fig. 1b).

Given the significant potential of this method, the purpose of this study is, therefore, to test, under controlled laboratory conditions, the adequacy of using PDMPO to estimate specific-growth rates of diatom species populations in the field. In particular, the main assumptions underlying the use of PDMPO in this context are tested for relevant (polar) diatom species covering a broad range in both shape, size, degree of silicification, and division rates.

Materials and procedures

Species selection and identification

Common (seasonally abundant) centric and pennate polar diatom species from multiple origins and with different characteristics were targeted in order to test for the reliability of the method. Based on previous experience from field test incubations with natural communities (Klaas, unpubl.), frustule size, shape and thickness can affect the signal intensity of the stain deposited and make recognition of stained valves in small ($< 10\,\mu$m) and thinly silicified species, for example, in the genus *Chaetoceros*, difficult. Frustule shape can also influence the quality of results, in particular for thin lanceolate needle-like diatoms such as *Pseudo-nitzschia* species, where girdle bands and valves cannot be readily distinguished using light/epifluorescence microscopy. Since during vegetative division, the production of the new valve can commence with the girdle bands in some species (Hildebrand et al. 2007), failure to distinguish these from the valves might lead to an overestimation of the number of newly divided cells (i.e., n_t' and n_t''), and, therefore, specific-growth rates.

In order to cover a broad range of key species-related frustule and life-cycle characteristic, three polar species showing steady growth over the acclimation period (see below) were selected for the experiments. These are: *Pseudo-nitzschia subcurvata* (strain 22_35) isolated by Bank Bezsteri and Lena Eggers (AWI) during Polarstern expedition PS117 on the northeastern margin of the Weddell Sea (59°3′S, 0°6′E); *Chaetoceros simplex* (strain CS 624, ANACC) isolated from the coastal waters of Antarctica (Prydz Bay) and kindly provided by Christel Hassler (University of Geneva, Switzerland), and *Thalassiosira* sp. (strain CC_Sed) originally identified as *T. hyalina*, collected during spring 2018 in the Kongsfjord, Svalbard and provided by Klara Wolf (AWI).

Culturing conditions

All species were grown in natural Antarctic (*P. subcurvata* and *C. simplex*) or Arctic (*Thalassiosira* sp.) seawater with nutrient addition to a final concentration of $100\,\mu$M nitrate, $100\,\mu$M silicic acid, and $6.25\,\mu$M phosphate, respectively, and proportionally enriched with vitamin and trace metals following the f/2 medium of Guillard and Ryther (1962). Culture media was sterile-filtered through a $0.2\,\mu$m capsule filter (Sartopore; Sartorius) and stored at 4°C before use.

Experiments and acclimation of strains were carried out in a temperature-controlled room set to 4°C. Temperature variability during acclimation and during experiments was monitored with a data logger submerged in a seawater-filled culture flask. During the whole acclimation and over the course of the experiment the recorded temperature was 4.0 ± 0.2°C.

Cultures and experiments were kept under a 16 : 8 h light : dark cycle at light intensities of $110 \pm 10\,\mu$mol photon m^{-2} s^{-1} or $20 \pm 3\,\mu$mol photon m^{-2} s^{-1}, depending on experiment. Light levels were adjusted and established using a light meter (ULM-500) equipped with a 4π-micro quantum sensor (Heinz Walz GmbH) submerged in a seawater-filled culture flask. Light was provided by four daylight lamps (LUMILUX DE LUXE, 6500K; Osram).

All species were grown in angle-necked polycarbonate culture flasks with hydrophobic membrane-filter caps to allow gas exchange. Bottles were laid flat, allowing minimum nutrient and light gradients, as well as maximum space for surface gas exchange.

Sampling and transfer of cultures were done in a clean bench, in sterile conditions, to avoid cross culture contamination. Before sampling, bottles were gently mixed at least 50 times to ensure homogeneous cell distribution in the culture media.

Experimental design

The main assumptions tested during this study were: (1) Addition of PDMPO does not affect division rates. (2) Newly divided cells (daughter cells) can be readily recognized by their fluorescent valves and PDMPO is taken up only in newly formed valves. (3) The populations do not divide synchronously (here the impact off light–dark cycles on division was also included). (4) The population of a single species in a natural assemblage has uniform specific-growth and mortality rates were not tested in this study but will be mentioned in our discussion.

Assumptions 1 and 2 were tested by comparing cell concentration-based growth rates with those based on PDMPO stain in control incubations and in incubations where PDMPO was added. This was carried out for *P. subcurvata*, *C. simplex*, and *Thalassiosira* sp. acclimated to $20\,\mu$mol photon m^{-2} s^{-1} at $0.125\,\mu$M (all species) and $0.6\,\mu$M (for *P. subcurvata* and *C. simplex*) PDMPO final concentrations. The impact of PDMPO addition was further tested on *Thalassiosira*

sp. acclimated at 110 μmol photon m^{-2} s^{-1} at both 0.125 and 0.6 μM PDMPO final concentration.

To ensure balanced growth and stable conditions, all cultures were acclimated in semi-continuous batch cultures for at least nine generations before starting the experiments. Following acclimation, the experimental incubations were similarly carried out in two consecutive phases: (1) To ensure that cells were acclimated and growing exponentially, cultures were transferred into new media at the end of the exponential growth phase for another nine generations (encompassing about three transfers in new media each). During this "acclimation phase" growth was monitored by measurements of in vivo chlorophyll *a* fluorescence using a TD700 fluorometer (Turner Designs). This method has been tested on several phytoplankton species yielding robust growth rate estimates provided measurements are carried out at the same time of day for each culture batch (Brand et al. 1981; Brand and Guillard 1981). (2) Following acclimation, cultures were diluted into 8 or 12 incubations bottles (replicate incubations) containing new media. In the first days after transfer, cell concentrations were monitored to ensure exponential growth. After this short period, PDMPO (LysoSensor Yellow/Blue DND-160; Thermo Fisher Scientific) was added to four or eight (depending on species and experiment) replicate bottles while the remaining four bottles were incubated without stain addition (controls). Experiments were terminated and sampled 24 h (full light–dark cycle) after PDMPO addition. Daily samples for cell enumeration, fixed with acidic Lugol's solution (around 1% final concentration), were taken during the control phase. After addition of PDMPO, samples for cell enumeration and PDMPO analysis were taken at the time of stain addition (t_0) and 24 h later (t_f). Further samples were taken at the beginning (if different from t_0) and end (if different from t_f) of both light and dark cycles, respectively. Samples were fixed with 2% (final concentration) hexamine-buffered formalin and stored in glass vials in the dark at 4°C until analysis.

To determine cell abundance, 10 mL of undiluted or diluted fixed sample (from three to four independent replicate bottles each) were settled in a 10 mL Utermöhl sedimentation chamber (HYDRO-BIOS; Utermöhl 1958; Edler 1979). Dilutions were carried out with seawater with either acidic Lugol's solution (1% final concentration) or hexamine-buffered formaldehyde solution (2% final concentration) depending on the chosen fixative of the sample. At least 300 cells were counted with a Zeiss Axiovert 40C inverted light microscope or a Zeiss Axiovert 200 epifluorescence microscope. Samples with PDMPO were counted with the aforementioned epifluorescence microscope equipped with a long pass filter (Zeiss Filter set 02; excitation: G365, beam splitter: FT395; emission: LP420). Samples were counted at ×200 to ×630 magnification depending on species and intensity of the PDMPO signal.

Growth rate estimations

Growth rates from cells counts were estimated using Eq. 1, while growth rates using PDMPO were calculated from the number of nonstained (n_t), half-stained (n'_t), and fully stained (n''_t) cells using Eq. 4 or 6. Cells attached to each other (potentially in the final phase of division) were also considered as nonstained, half-stained, and fully stained individuals, respectively, based on the presence/absence of a PDMPO signal on the valves. The presence of nonstained frustules in the sample determined the choice of Eq. 4 over Eq. 6. In all cases, unstained cell which were dead (empty frustules) or appeared as empty half frustules, were noted, but excluded from the count as their contribution to population growth was unlikely. Such "dead" cells were uncommon in the samples ($\ll 1\%$). All estimated specific-growth rates are given in the Supplementary Table S1.

Data analysis

All statistical data analysis was carried out with R (version 4.0.1; 2020-2106-06). Assessment of differences in growth rate based on the evolution of cell concentrations (μ_{cc}) over a 24-h period and growth rates based on PDMPO stain pattern (i.e., number of unstained, half-stained, and fully stained frustules) 24 h after PDMPO addition (μ_{PDMPO}) were performed using one-way ANOVA with $\alpha = 0.05$, followed by Tukey's honestly significant difference post hoc test. Further Welch's *t*-test ($\alpha = 0.05$) and Bayesian *t*-test (B$_{10} > 3.16$) were used as robust *t*-tests. Prior to ANOVA a Levene's test for homogeneity was applied, ensuring homoscedasticity of the variables to meet the prerequisite for the test. If data variances were not homogeneous, Welch's ANOVA ($\alpha = 0.05$) and Games–Howell post hoc test were applied to yield adequate statistical estimates.

Both tests, *t*-test and ANOVA, were also applied to determine treatment effects of the different PDMPO concentrations and light settings, as well as testing for day–night cycles in division rates by comparing specific-growth rates estimated for the full light–dark cycle (24-h incubation) and the 8-h dark cycle.

Assessment

Strain acclimation

During acclimation, cell concentrations were monitored through in vivo fluorescence (IVF), while during the "control phase" of the experiments both IVF and cell counts were carried out (data not shown). Comparison of growth rates based on IVF (μ_{FSU}) for all acclimated cultures showed similar rates during acclimation and control phases. However, during the control phase, μ_{FSU} and cell concentration-based growth rates (μ_{cc}) showed significant differences (*P. subcurvata* 20 μmol photon m^{-2} s^{-1} one-way ANOVA: $F_{1,18} = 21.04$, $p < 0.001$; *C. simplex* 20 μmol photon m^{-2} s^{-1} one-way ANOVA: $F_{3,18} = 35.18$, $p < 0.001$; *Thalassiosira* sp. 20 μmol photon
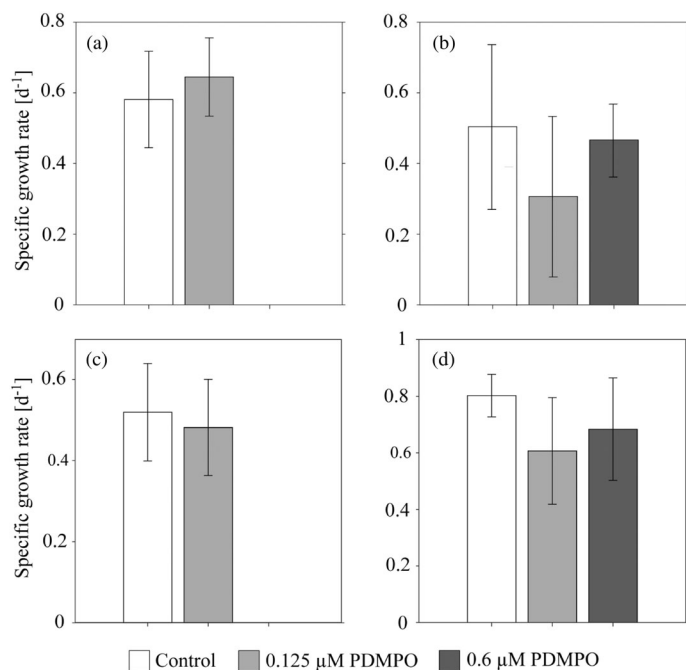
Fig. 2. Mean specific-growth rates estimated from cell abundance changes over 24 h (μ_{cc}) in controls and corresponding PDMPO incubations for (**a**) *Pseudo-nitzschia subcurvata*, (**b**) *Chaetoceros simplex*, and (**c**) *Thalassiosira.* sp. grown at 20 μmol photon m^{-2} s^{-1} and (**d**) *Thalassiosira* sp. grown at 110 μmol photon m^{-2} s^{-1}. Error bars represent one standard deviation. Values and number of replicates for each estimate are also given in Supplementary Table S1.

Fig. 3. Average specific-growth rates estimated from cell abundance changes over 24 h (white bars, μ_{cc}) and from PDMPO staining counts (gray bars, μ_{PDMPO}) from incubations with 0.125 μM (left panels) and 0.6 μM (right panels) PDMPO for (**a**, **b**) *Pseudo-nitzschia subcurvata*; (**c**, **d**) *Chaetoceros simplex*; (**e**, **f**) *Thalassiosira* sp. grown at 110 μmol photon m^{-2} s^{-1} and (**g**) *Thalassiosira* sp. at 20 μmol photon m^{-2} s^{-1}. Error bars represent one standard deviation. Values and number of replicates for each estimate are also given in Supplementary Table S1.

m^{-2} s^{-1} one-way ANOVA: $F_{1,13}$ = 19.09, p = 0.001; *Thalassiosira* sp. 110 μmol photon m^{-2} s^{-1} Welch's ANOVA: $F_{6,9}$ = 3.65, p = 0.04) with generally lower values for μ_{FSU}. Hence, while IVF might still be a useful quick method to follow the growth stages in phytoplankton cultures (Brand et al. 1981; Brand and Guillard 1981), this method might, in some cases, underestimate their specific-growth rates.

Impact of PDMPO on growth rates

Specific-growth rates estimated over the 24-h incubations based on cell concentration (μ_{cc}, Eq. 2) for control bottles and bottles with different additions of PDMPO (0.125 and 0.6 μM, respectively) at 20 and 110 μmol photon m^{-2} s^{-1} light intensity, are shown in Fig. 2 and in the Supplementary Table S1.

Specific-growth rates of *P. subcurvata* at 20 μmol photon m^{-2} s^{-1} in the control incubations and in the treatment with 0.125 μM PDMPO showed no significant differences (Welch's *t*-test, t = −0.63, df = 3.84, p = 0.57; Bayesian *t*-test, B_{10} = 0.54). For this species, an incubation at 0.6 μM PDMPO final concentration was also carried out, however, no samples for cell counts were collected at t = 0. The impact of 0.6 μM PDMPO addition is unlikely to be significant either, since the PDMPO estimated specific-growth rates (μ_{PDMPO}, Fig. 3, and text below) did not differ statistically from the control incubations without any PDMPO addition or the incubation with
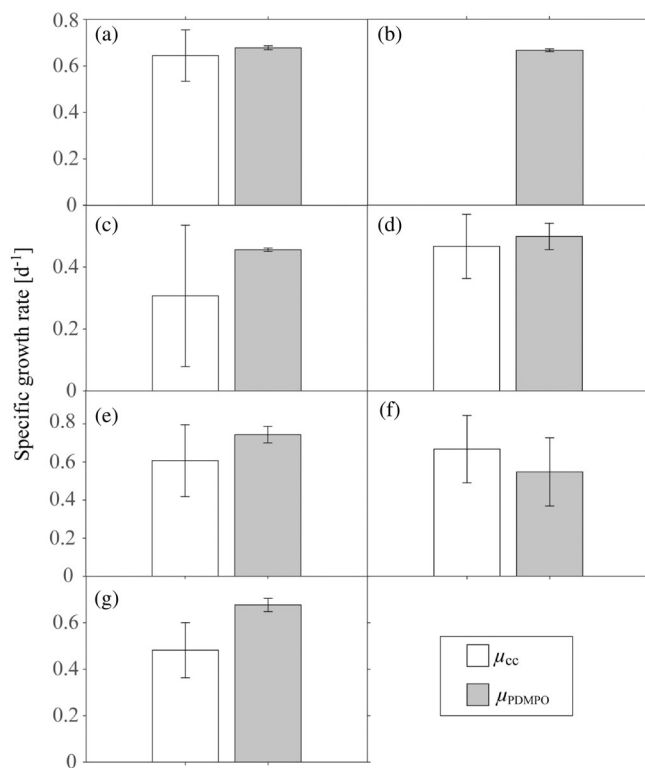
0.125 μM PDMPO addition. Incubations with *C. simplex* showed larger variability in specific-growth rates in all treatments (Fig. 2b) with no significant differences between treatments (one-way ANOVA, $F_{2,6}$ = 0.85, p = 0.47). It should be noted that the high variability derives from one replicate with low specific-growth rates in the control and 0.125 μM PDMPO treatment, respectively. The specific-growth rates between control incubations and the 0.125 μM PDMPO treatments without outliers (0.639 d^{-1} and 0.642 d^{-1} in the control and 0.502 d^{-1} and 0.363 d^{-1} at 0.125 μM PDMPO, respectively) and the 0.6 μM PDMPO treatment 0.438–0.539 d^{-1}could indicate some negative effect of PDMPO on specific-growth rates in *C. simplex*. The more robust specific-growth rates based on staining patterns (μ_{PDMPO}, Fig. 3d), however, did not differ 0.125 and 0.6 μM PDMPO addition (see also text below on PDMPO-derived specific-growth rates).

On average, controls and both treatments of *Thalassiosira* sp. at 110 μmol photon m^{-2} s^{-1} grew with a 34% higher rate than the same strain grown at 20 μmol photon m^{-2} s^{-1}, although this difference was overall not statistically significant (one-way ANOVA, $F_{4,13}$ = 2.74, p = 0.07). The lack of

statistical difference between treatments at 20 and 110 μmol photon m^{-2} s^{-1} is, however, possibly due to the high variability of cell counts and derived specific-growth rates in the 0.125 μM PDMPO treatments at 110 μmol photon m^{-2} s^{-1} (Fig. 2c,d). Welch's *t*-test showed that specific-growth rates in the controls (with the least variability) were significantly higher at 110 μmol photon m^{-2} s^{-1} (0.80 $\pm$ 0.06 d^{-1}; Fig. 2d) as compared to growth in the control treatment at 20 μmol photon m^{-2} s^{-1} (0.52 $\pm$ 0.12 d^{-1}; Fig. 2c; $t = 3.60$, df $= 3.17$, $p = 0.03$, Bayesian *t*-test, B$_{10} = 5.52$). Comparison of specific-growth rates in controls and PDMPO treatments for both light intensities did not indicate an effect of PDMPO concentration (at 20 μmol photon m^{-2} s^{-1}: Welch's *t*-test $t = (0.38)$, df $= 4.0$, $p = 0.72$; Bayesian *t*-test B$_{10} = 0.49$; and for 110 μmol photon m^{-2} s^{-1}: one-way ANOVA, $F_{2,9} = 1.57$, $p = 0.26$).

In summary, addition of PDMPO up to 0.6 μM final concentrations did not seem to affect the rates of cell division for any of the species tested within the 24-h incubations carried out in this study.

PDMPO-derived specific-growth rates

Specific-growth rates obtained from the evolution of cell concentration (μ_{cc}, Eq. 2) and from the abundance of PDMPO unstained, half, and fully stained cells after 24-h incubation (μ_{PDMPO}, Eq. 4) estimated for the treatments with 0.125 and 0.6 μM final PDMPO concentration are shown in Fig. 3 and Supplementary Table S1. For *P. subcurvata* cells lying on their valve face (around 20% of total cells counted) it was not possible to determine unequivocally if cells were half or fully stained (Fig. 4a). The presence of unstained cells indicated, however, that while most cells had divided once, the incubation period of 24 h did not exceed one generation time. In addition, all dividing cells observed in the samples (Fig. 4b–d) were only half-stained, a further indication that all stained cells had divided only once. As a consequence, all cells lying on their valve face and showing a PDMPO signal were considered half-stained. The resulting specific-growth rate estimate (μ_{PDMPO}) was not significantly different from the rates estimated through the evolution of cell concentrations (μ_{cc}) for the 0.125 μM treatment (Fig. 3a; Welch's *t*-test: $t = -0.518$, df $= 2.02$, $p = 0.656$; Bayesian *t*-test: B$_{10} = 0.51$). Furthermore, no difference was found between μ_{PDMPO} at 0.6 μM (Fig. 3b and Supplementary Table S1) and values (μ_{cc} and μ_{PDMPO}) for the 0.125 μM treatment (Fig. 3a) as well as specific-growth rates in the control treatment (Fig. 2a; one-way ANOVA, $F_{3,9} = 0.90$, $p = 0.48$). These results indicate that our assumptions that (1) all cells with a PDMPO signal were only half-stained and (2) 0.6 μM PDMPO addition does not affect rates of cell division for *P. subcurvata*, are valid. Furthermore, our observation of the staining pattern in dividing cells indicates that new valves are formed before or simultaneously with the gridle bands. This also applies to the other species studied here.

For *C. simplex* average PDMPO-based specific-growth rates (μ_{PDMPO}) were somewhat higher (up to 33%) than μ_{cc} (Fig. 3c,d). However, given the higher uncertainties in μ_{cc}, both did not differ significantly. Overall, no significant difference in specific-growth rates estimates or treatment were found for *C. simplex* (one-way ANOVA, $F_{3,8} = 1.35$, $p = 0.33$).

In contrast to the other species, our *Thalassiosira* sp. strain showed the presence of nonstained, half-stained, and fully stained cells, indicating that after 24 h, some cell had not divided yet, while other had already undergone two division cycles (Fig. 4e). Hence, this strain did not show homogenous cell division rates.

Furthermore, two different size classes of cells were observed (Fig. 4e), as well as auxospore formation (Fig. 4f). Fully stained cells were also observed in all size classes. These observations indicate that the strain had undergone sexual reproduction and was not monoclonal. SEM observations did, however, indicate that the culture was monospecific. The PDMPO-based specific-growth rates (μ_{PDMPO}) presented here correspond to the population specific-growth rate, which is the estimate matching those based on the changes in cell numbers (μ_{cc}).

No statistical difference was found between μ_{cc} (0.61 $\pm$ 0.19 d^{-1}) and μ_{PDMPO} (0.74 $\pm$ 0.04 d^{-1}) for *Thalassiosira* sp. grown at 110 μmol photon m^{-2} s^{-1} and 0.125 μM PDMPO addition (Welch's *t*-test $t = 1.40$, df $= 3.41$, $p = 0.25$; Bayesian *t*-test, B$_{10} = 0.71$; Fig. 3e). In the 0.6 μM PDMPO treatment (Fig. 3f), μ_{cc} was also similar to μ_{PDMPO} (Welch's *t*-test $t = 0.95$, df $= 6.0$, $p = 0.38$; Bayesian *t*-test, B$_{10} = 0.58$). Differences between both PDMPO treatments (0.125 and 0.6 μM PDMPO) and specific-growth rate estimates (μ_{cc} and μ_{PDMPO}) were not significant (one-way ANOVA, $F_{3,11} = 0.82$, $p = 0.512$). At 20 μmol photon m^{-2} s^{-1} and 0.125 μM PDMPO addition, μ_{PDMPO} of *Thalassiosira* sp. was about 30% higher than μ_{cc}; but only marginally statistically different (Fig. 3g; Welch's *t*-test $t = 2.77$, df $= 2.23$, $p = 0.10$; Bayesian *t*-test, B$_{10} = 2.13$). Finally, as for the control incubations, specific-growth rates in the 0.125 μM treatment estimated from PDMPO (μ_{PDMPO}) were higher at 110 μmol photon m^{-2} s^{-1} than at 20 μmol photon m^{-2} s^{-1} (0.68 $\pm$ 0.03 and 0.74 $\pm$ 0.04, respectively) albeit not significantly (Fig. 3e,g; Welch's *t*-test $t = 2.25$, df $= 3.47$, $p = 0.10$; Bayesian *t*-test, B$_{10} = 1.51$).

Daily specific-growth rate variability

In order to examine variability in division rates due to phasing of mitosis by light–dark cycles, specific-growth rates were also determined for the duration of the dark cycle (8 h) for all species in experiments with 0.125 μM PDMPO addition (Fig. 5). Generally, the variability in specific-growth rates determined from changes in cell concentrations was higher than those determined from PDMPO counts (Fig. 5). This was especially noticeable for values estimated during the dark cycle, which represents a much shorter duration (8 h) than the full day–night 24-h cycle. As a consequence, no significant
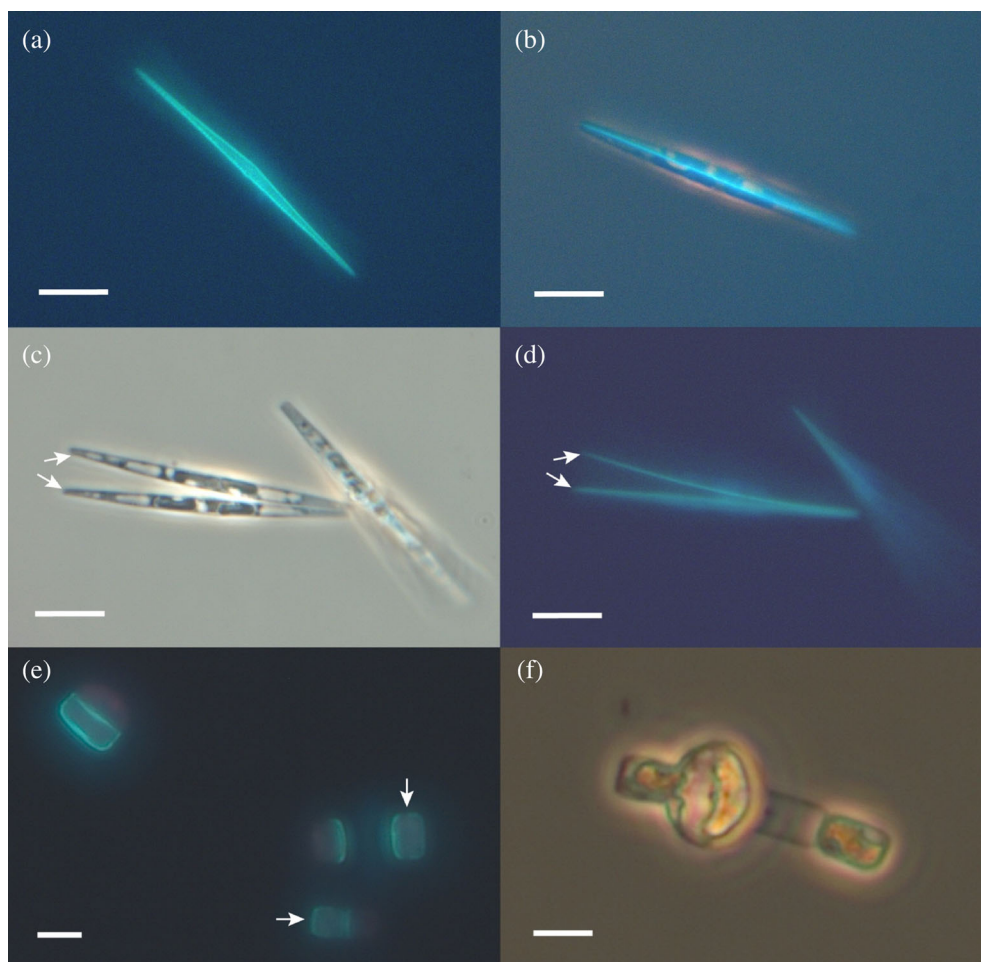
Fig. 4. *Pseudo-nitzschia subcurvata* incubated at 0.6 μM PDMPO final concentration showing (**a**) fluorescent PDMPO stained cell lying on the valve face and (**b–d**) dividing cells with PDMPO incorporation in the newly forming valves (**b** and **d**). Cells shown in panel **d** (epifluorescence) are the same as in panel **c** (phase contrast), white arrows indicate the newly formed valves. *Thalassiosira* sp. cells (**e**) with fluorescent PDMPO stained valves showing the different size classes of cells as well as fully stained (indicated by the white arrows) and half-stained cells. (**f**) Auxospore formation in *Thalassiosira* sp. White scale bars in all panels correspond to 10 μm.

differences were found in mean specific-growth rates determined from changes in cell concentrations (μ_{cc}) between the dark cycle and estimates over the whole light–dark (24 h) cycle for any of the species studied here (Fig. 5a,c,e). Specific-growth rates (μ_{PDMPO}) estimated from the counts of PDMPO staining, however, revealed a significant difference in division rates between the dark cycle and the entire light–dark cycle for all species (Fig. 5b,d,f): *P. subcurvata* (Welch's *t*-test $t = 6.41$, df $= 2.04$, $p = 0.02$; Bayesian *t*-test $B_{10} = 14.0$) showed division rates on average 47% higher during the dark phase. For *C. simplex* division rates where twice as high (98% average) during the dark phase (Welch's *t*-test $t = 7.55$, df $= 2.01$, $p = 0.02$; Bayesian *t*-test $B_{10} = 21.5$). *Thalassiosira* sp. also divided preferentially during the dark phase although not as markedly as the other species (23% higher rates). Differences between dark and full light–dark cycles were nevertheless also significantly different for this species

(Fig. 5e; Welch's *t*-test $t = -4.23$, df $= 2.99$, $p = 0.02$; Bayesian *t*-test $B_{10} = 5.1$).

Discussion

The comparison of in situ specific-growth rates of all species in experiment estimated through cell concentration changes (μ_{cc}) and PDMPO staining (μ_{PDMPO}) indicates that the addition of PDMPO up to 0.6 μM final concentration does not negatively affect division rates of *P. subcurvata*, and *Thalassiosira* sp within a 24-h incubation period. No significant differences were found for *C. simplex* either, however, given the large variability in μ_{cc} in the control incubations and at 0.125 μM PDMPO, due in both cases to one replicate with low specific-growth rates, a negative effect of 0.125 μM PDMPO on specific-growth rates cannot be ruled out. Counting of the fixed samples stained with PDMPO took place
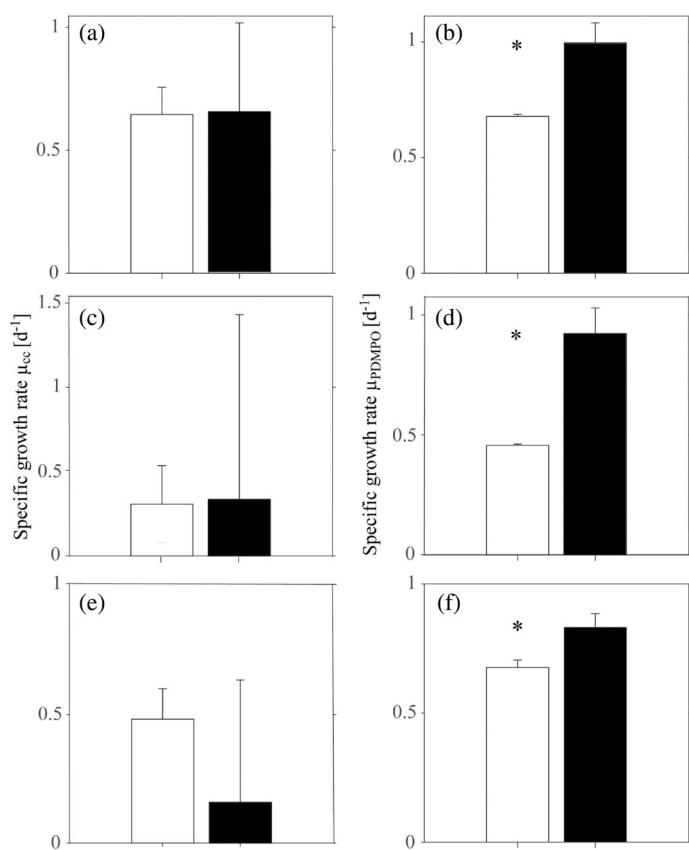
Fig. 5. Average specific-growth rate estimated over 24 h (light and dark cycle, white bars) and during the dark cycle (8 h, black bars) calculated from the evolution of cell concentrations (μ_{cc}; left panels) and from the PDMPO staining counts (μ_{PDMPO}; right panels) for (**a, b**) *Pseudo-nitzschia subcurvata*; (**c, d**) *Chaetoceros simplex*; (**e, f**) *Thalassiosira* sp. grown at 20 μmol photon m^{-2} s^{-1} with 0.125 μM PDMPO addition. Asterisk * indicates significant difference between specific-growth rates over 24 h and over the dark (8 h) cycle, respectively. Error bars correspond to one standard deviation. Values and number of replicates for each estimate are also given in Supplementary Table S1.

2 months after collection for the 0.125 μM PDMPO incubations and after up to 1 year for the *P. subcurvata* experiments with 0.6 μM PDMPO. In all cases, the fluorescent stain intensity was well preserved.

Comparison of μ_{cc} and μ_{PDMPO} shows that the PDMPO-based method provides reliable estimates of species specific-growth rates. Furthermore, μ_{PDMPO} tended to be substantially less variable than μ_{cc}: standard deviation values for μ_{PDMPO} were around 1% of the mean specific-growth rate estimated after the 24-h incubations for *P. subcurvata*, 1–9% for *C. simplex* and somewhat higher for *Thalassiosira* sp. (4–32%). Values for the shorter dark (8 h) cycle ranged from 7% to 12% of the mean for all species. For μ_{cc}, values were markedly higher but also more variable (17–74% for rates determined after 24-h incubation and higher during the shorter dark cycle). These differences can be explained by several factors: (1) Estimating μ_{cc} requires counting two sets of samples (start

and end of the incubation), as opposed to one set of (final) samples for μ_{PDMPO}, with all the variability that accumulates due to differences between replicates for each set, sampling errors and counting errors. (2) Moreover, errors during sampling are more likely to affect estimates of cell concentrations rather than the relative abundance in nonstained, half-stained, and fully stained cells. (3) Finally, the relative abundance in nonstained, half-stained, and fully stained cells is not likely to be affected by mortality. In the case of the experiments presented here, mortality was not a significant concern, as empty (dead) cells were rarely found in the samples. In incubations with natural communities, however, this is one significant advantages of the method. As mentioned previously, standard deviations of μ_{PDMPO} for *Thalassiosira* sp. were higher than for the other species, in particular for the treatment with 0.6 μM PDMPO addition at 110 μmol photon m^{-2} s^{-1} (Fig. 3). This can be attributed to the high variability in counts of unstained cells in our four independent replicate incubations: unstained cells contributed 3%, 4%, 29%, and 50% of total cell counts (around 400 cells counted in each case), respectively, leading to a range in μ_{PDMPO} between 0.33 and 0.72 d^{-1}. Duplicate counts for the samples with the lowest μ_{PDMPO} due to the highest contribution of unstained cells (29% and 50%), did not change the results significantly for these samples. These variations, and the resulting lower average μ_{PDMPO} estimate for this treatment compared to the other experiments with *Thalassiosira* sp. point toward larger variability in growth rates within replicate incubations (not seen for μ_{cc}), or an error during sampling of the experiments (uneven sampling). Hence, while this method is more robust, we still recommend replicate incubations and care should be taken while sampling.

In addition to being less variable and prone to errors, with the exception of the treatment mentioned above (*Thalassiosira* sp. with 0.6 μM PDMPO addition at 110 μmol photon m^{-2} s^{-1}), μ_{PDMPO} tended to be higher than μ_{cc} for all species tested. This effect was more pronounced for estimates encompassing the dark cycle. Values of μ_{PDMPO} where higher by 5% (24-h cycle) and 34% (dark cycle) for *P. subcurvata*, 6–33% (24-h cycle) and 64% (dark cycle) for *C. simplex*, and 18–29% (24-h cycle) and 81% (dark cycle) for *Thalassiosira* sp. These patterns are likely related to the identification/interpretation of the number of cells in dividing doublets (such as illustrated in Fig. 4b for *P. subcurvata*) where the presence of a PDMPO signal for the newly formed valves leads to a more robust identification of the presence of one or two cells in dividing doublet and consequently higher relative numbers of divided cells and growth rates.

Field application

Tracers for Si incorporation in diatom frustules, including fluorescent dyes such as PDMPO, have been previously used in both laboratory and field studies to investigate silicification and quantify silicon uptake in diatoms (Brzezinski and

Conley 1994; Shipe et al. 1999; Shimizu et al. 2001; Leblanc and Hutchins 2005; Znachor and Nedoma 2008; McNair et al. 2015, 2018*a*,*b*), and in a few cases, to estimate in situ species specific-growth rates (Shipe et al. 1999; McNair et al. 2018*a*,*b*). Previous studies using PDMPO staining patterns (McNair et al. 2018*a*,*b*) relied on different approaches with different sets of assumptions, depended on species characteristics (chain forming vs. single cells, slow vs. fast-growing), to attribute and estimate division rates of diatom species in the field. In the present study, we provide for the first time (1) the theoretical background and mathematical expression universally applicable to the study of diatom division rates based on frustule staining patterns; (2) a test of the method including assumptions and caveats. Leblanc and Hutchins (2005) tested the use of 0.125 μM PDMPO final concentration on the fluorescent signal as well as the potential toxicity of PDMPO over a range of final concentrations between 0.1 and 1 μM in natural diatom assemblages incubated for 48 and 96 h. Their study shows strong signal at concentrations as low as 0.125 μM, and potential toxicity effect after 48-h incubation with 0.5 and 1 μM final PDMPO concentration. Our results confirmed that the use of 0.125 μM final concentration, provides sufficient signal even for small *Chaetoceros* species. It should be noted, however, that our experiments were carried out in nutrient-replete conditions (in particular trace metals and Si). Preliminary observations using natural Southern Ocean communities (Klaas, unpubl.), indicates that under natural conditions, using higher concentrations might be warranted. McNair et al. (2015, 2018*b*) successfuly applied a concentration of 0.157 μM to study Si uptake in a wide range of species from natural assemblages. Based on these previous studies and our experiments, indicating that, for shorter (24 h) incubation times, concentrations of up to 0.6 μM did not significantly affect division rates of the species tested (belonging to three different genera); higher concentrations in the range of 0.2 μM (Leblanc and Hutchins 2005; McNair et al. 2015; this study) should give a reliable signal without affecting growth rates in natural assemblages.

Our study further confirms that the illumination cycle significantly influences the timing of division in diatoms, highlighting the importance of extending incubation periods to include both light and dark cycles in order to obtain reliable estimates of in situ growth rates.

One of the main caveats of the method is, for some species, the difficulty in discriminating between half-stained and fully stained cells using conventional microscopy methods. This is particularly relevant for nonchain-forming discoid diatoms (*Coscinodiscus*, some *Thalassiosira* species to name a few) and pennate diatoms which typically lie on their valve face when settled for counting. This is compounded by the fact that natural diatom populations could show significant intraspecific variability in growth rates (Brand et al. 1981; Sjöqvist and Kremp 2016; Wolf et al. 2018). These limitations can be overcome by using 3D imaging techniques (Leblanc and
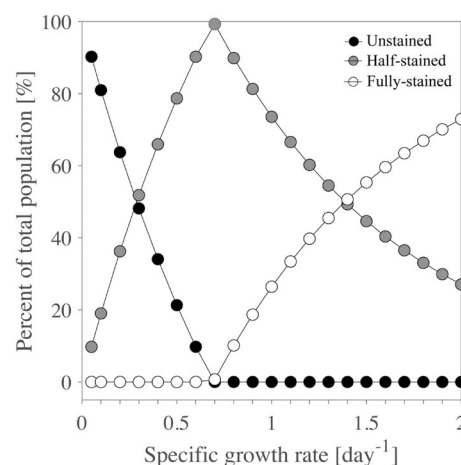

Fig. 6. Percent contribution of unstained, half-stained, and double-stained cells as a function of specific-growth rate after a 24-h incubation with PDMPO.

Hutchins 2005; McNair et al. 2015, 2018*b*), or reducing the incubation length to below one generation time, ensuring the absence of double-stained cells. For species with specific-growth rates exceeding 0.69 d^{-1} (one doubling every day), this can also be achieved by increasing the temporal sampling resolution (i.e., taking a time-series over a full light–dark cycle or parallel incubations covering a full light and a full dark cycle, respectively). The advantage of the later is to provide further information on phasing of division as well as the potential variability in growth rates within a species population. Furthermore, new development of vital stains, with different excitation and emission spectra, higher quantum yields could help overcome these caveats in the future (Annenkov et al. 2018).

Within the expected range of specific-growth rates of an actively growing diatom species population in natural assemblages and conditions (0.1–1.5 d^{-1} corresponding to a range between one division a week and two divisions a day; Eppley 1981; Behrenfeld et al. 2013; Laws 2013; McNair et al. 2018*a*) robust specific-growth rates estimates based on 24-h incubations, would critically depend on the staining patterns, in itself dependent on the species division rates (Fig. 6), as well as number of cells counted for each species. The uncertainties associated with both these variables can be estimated from the fact that the probability to count unstained and half-stained cells for division rates slower than the incubation period and the probability to count half-stained and fully stained cells for division rates faster than the incubations period follow binomial distributions (see Supporting Information S1). Based on the above, uncertainties for μ as a function of the number of cells counted can be estimated by Monte Carlo simulations (Fig. 7). The obtained coefficients of variations for μ indicate that for 24-h incubations a good resolution and errors of around 10% can be obtained when counting at least 25 cells (Fig. 7a) for species dividing at rates faster than
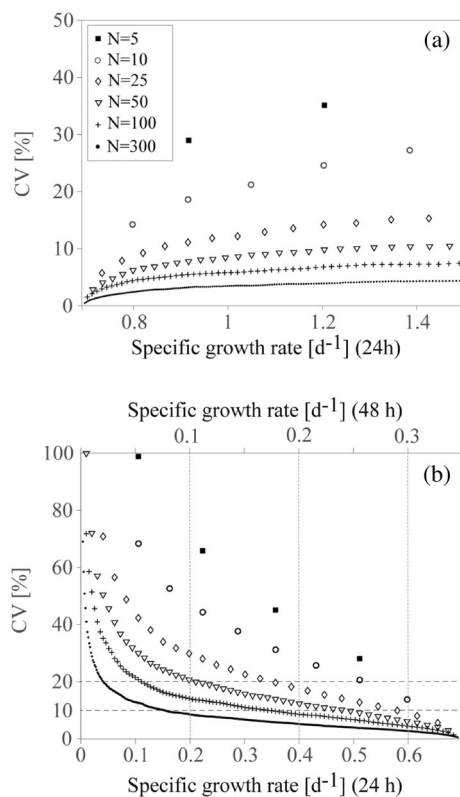
Fig. 7. Uncertainty of specific-growth rates estimates given as percent coefficient of variation (CV) as a function of number of cells counted (*N*) and specific-growth rates for (**a**) species growing at rates > 0.69 d^{-1} after a 24-h incubation with PDMPO, and (**b**) species growing at rates < 0.69 d^{-1} after 24 h (lower *x*-axis) incubation with PDMPO and species growing at rates < 0.35 d^{-1} after 48 h (upper *x*-axis) incubation with PDMPO.

0.69 d^{-1}. For slower growing species (0.4–0.69 d^{-1}) larger cell counts (≤ 50 cells) are necessary, due to the low proportion of half-stained cells (Fig. 7b). This caveat of the method can be overcome by extending the incubation time (Fig. 7b).

An incubation period of 2 d reduces the error in specific-growth rates estimates to a range between 10% and 20% at 25 cells counted for specific-growth rates between 0.2 and 0.35 d^{-1} (Fig. 7b).

Hence, for mixed natural assemblages, protocols (incubation time and number of cells counted per species) should be adapted depending on the study focus. Finally, it should be noted that low cell counts (< 10 cells) significantly reduce the resolution, given that the number of possible outcomes μ_i (with $i = 1, 2, 3, ..., N$) is equal to N the number of cells counted.

Comments and recommendations

The application of PDMPO to estimate species specific-growth rates is shown to provide reliable and robust results within a short (24 h) incubation time frame: the method is

mortality independent, less variable than previous approaches and the short incubation time limits the impact of the so-called "bottle" effects. The number of cells counted per species present in natural mixed assemblages, can present a significant bottleneck in the application of the method. Our uncertainty estimates, indicates that 48-h incubations with sampling after 24 h for the faster growing species (reducing bottle effects) and sampling after 48 h for slower (approximately < 0.4 d^{-1}) growing species might be more appropriate for a good coverage of species specific-growth rates in field studies. The proposed standard concentration of 0.125 μM PDMPO is sufficient to stain weakly silicified diatoms under replete nutrient conditions. However, even a higher concentration (up to 0.6 μM final PDMPO concentrations) does not significantly impair growth rates within a 24-h incubation time. Given the limited number of species tested so far, and the variability in nutrient conditions in the field (in particular Si and trace-metal concentrations that might affect Si-deposition and PDMPO incorporation in frustules) somewhat higher PDMPO concentrations (0.157–0.2 μM) might be warranted. Our results, as well as previous observations, indicate that phasing of cell division by the illumination cycle is a common feature in diatoms and highlights the importance of covering the full light–dark cycle when estimating population growth and associated parameters. While the PDMPO technique does not allow to estimate the individual growth rates of genetically diverse species populations, the method still provides a robust estimate of the species population growth rate as well as, depending on sampling strategy, information on the variability of growth rates within the population.

References

Abelmann, A., R. Gersonde, G. Cortese, G. Kuhn, and V. Smetacek. 2006. Extensive phytoplankton blooms in the Atlantic sector of the glacial Southern Ocean. Paleoceanography **21**: 1–9. doi:10.1029/2005PA001199

Annenkov, V. V., S. N. Zelinskiy, V. A. Pal'shin, T. N. Avezova, and E. N. Danilovtseva. 2018. Vital fluorescent dyes for study of silicifying organisms. Limnol. Freshw. Biol. **1**: 74–80. doi:10.31951/2658-3518-2018-AA-1-74

Assmy, P., V. Smetacek, M. Montresor, and others. 2013. Thick-shelled, grazer-protected diatoms decouple ocean carbon and silicon cycles in the iron-limited Antarctic circumpolar current. Proc. Natl. Acad. Sci. USA **110**: 20633–20638. doi:10.1073/pnas.1309345110

Behrenfeld, M. J. 2010. Abandoning Sverdrup's critical depth hypothesis on phytoplankton blooms. Ecology **91**: 977–989. doi:10.1890/09-1207.1

Behrenfeld, M. J., S. C. Doney, I. Lima, E. S. Boss, and D. A. Siegel. 2013. Annual cycles of ecological disturbance and recovery underlying the subarctic Atlantic spring plankton bloom. Glob. Biogeochem. Cycles **27**: 526–540. doi:10.1002/gbc.20050

Bowler, C., A. Vardi, and A. E. Allen. 2010. Oceanographic and biogeochemical insights from diatom genomes. Ann. Rev. Mar. Sci. **2**: 333–365. doi:10.1146/annurev-marine-120308-081051

Brand, L. E. 1989. Review of genetic variation in marine phytoplankton species and the ecological implications. Biol. Oceanogr. **6**: 397–409. doi:10.1080/01965581.1988.10749542

Brand, L. E., and R. R. L. Guillard. 1981. The effects of continuous light and light intensity on the reproduction rates of twenty-two species of marine phytoplankton. J. Exp. Mar. Bio. Ecol. **50**: 119–132. doi:10.1016/0022-0981(81)90045-9

Brand, L. E., L. S. Murphy, and R. R. L. Guillard. 1981. Genetic variability and differentiation in the temperature niche component of the diatom *Thalassiosira pseudonana*. Mar. Biol. **62**: 103–110. doi:10.1007/BF00388171

Brzezinski, M. A., and D. J. Conley. 1994. Silicon deposition during the cell cycle of Thalassiosira weissflogii (Bacillariophycae) determined using dual rhodamine 123 and propidium iodide staining. J. Phycol. **30**: 45–55. doi:10.1111/j.0022-3646.1994.00045.x

Chisholm, S. W., and L. E. Brand. 1981. Persistence of cell division phasing in marine phytoplankton in continuous light after entrainment to light: Dark cycles. J. Exp. Mar. Bio. Ecol. **51**: 107–118. doi:10.1016/0022-0981(81)90123-4

Edler, L. 1979. Recommendations on methods for marine biological studies in the Baltic Sea. Phytoplankton and chlorophyll. Mar. Biol. **5**: 1–38.

Eppley, R. W. 1981. Relations between nutrient assimilation and growth in phytoplankton with a brief review of estimates of growth rate in the ocean. Can. Bull. Fish. Aquat. Sci. **210**: 251–263.

Eppley, R. W., R. W. Holmes, and E. Paasche. 1967. Periodicity in cell division and physiological behavior of *Ditylum brightwellii*, a marine planktonic diatom, during growth in light–dark cycles. Arch. Mikrobiol. **56**: 305–323. doi:10.1007/BF00425206

Guillard, R. R. L., and J. H. Ryther. 1962. Studies of marine planktonic diatoms: I. *Cyclotella nana* Hustedt, and *Detonula confercavea* (cleve) gran. Can. J. Microbiol. **8**: 229–239. doi:10.1139/m62-029

Hildebrand, M., L. G. Frigeri, and A. K. Davis. 2007. Synchronized growth of *Thalassiosira pseudonana* (Bacillariophyceae) provides novel insights into cell-wall synthesis processes in relation to the cell cycle. J. Phycol. **43**: 730–740. doi:10.1111/j.1529-8817.2007.00361.x

Hildebrand, M., S. J. L. Lerch, and R. P. Shrestha. 2018. Understanding diatom cell wall silicification—Moving forward. Front. Mar. Sci. **5**: 125. doi:10.3389/fmars.2018.00125

Laws, E. A. 2013. Evaluation of in situ phytoplankton growth rates: A synthesis of data from varied approaches. Ann. Rev. Mar. Sci. **5**: 247–268. doi:10.1146/annurev-marine-121211-172258

Leblanc, K., and D. A. Hutchins. 2005. New applications of a biogenic silica deposition fluorophore in the study of oceanic diatoms. Limnol. Oceanogr.: Methods **3**: 462–476. doi:10.4319/lom.2005.3.462

Li, C. W., and B. E. Volcani. 1985. Studies on the biochemistry and fine structure of silica shell formation in diatoms. IX. Sequential valve formation in a centric diatom, *Chaetoceros rostratum*. Protoplasma **124**: 30–41. doi:10.1007/BF01279721

McDuff, R. E., and S. W. Chisholm. 1982. The calculation of in situ growth rates of phytoplankton populations from fractions of cells undergoing mitosis: A clarification. Limnol. Oceanogr. **27**: 783–788. doi:10.4319/lo.1982.27.4.0783

McNair, H. M., M. A. Brzezinski, and J. W. Krause. 2015. Quantifying diatom silicification with the fluorescent dye, PDMPO. Limnol. Oceanogr.: Methods **13**: 587–599. doi:10.1002/lom3.10049

McNair, H. M., M. A. Brzezinski, and J. W. Krause. 2018*a*. Diatom populations in an upwelling environment decrease silica content to avoid growth limitation. Environ. Microbiol. **20**: 4184–4193. doi:10.1111/1462-2920.14431

McNair, H. M., M. A. Brzezinski, C. P. Till, and J. W. Krause. 2018*b*. Taxon-specific contributions to silica production in natural diatoms assemblage. Limnol. Oceanogr. **63**: 1056–1075. doi:10.1002/lno.10754

Nelson, D. M., and L. E. Brand. 1979. Cell division periodicity in 13 species of marine phytoplankton on a light: Dark cycle. J. Phycol. **15**: 67–75. doi:10.1111/j.1529-8817.1979.tb02964.x

Nelson, D. M., P. Tréguer, M. A. Brzezinski, A. Leynaert, and B. Queguiner. 1995. Production and dissolution of biogenic silica in the ocean - revised global estimates, comparison with regional data and relationship to biogenic sedimentation. Glob. Biogeochem. Cycles **9**: 359–372. doi:10.1029/95GB01070

Oh, H. S., S. E. Lee, C. S. Han, and others. 2018. Silicon transporter genes of *Fragilariopsis cylindrus* (Bacillariophyceae) are differentially expressed during the progression of cell cycle synchronized by si or light. Algae **33**: 191–203. doi:10.4490/algae.2018.33.5.8

Owens, T. G., P. G. Falkowski, and T. E. Whitledge. 1980. Diel periodicity in cellular chlorophyll content in marine diatoms. Mar. Biol. **59**: 71–77. doi:10.1007/BF00405456

Pelusi, A., F. Margiotta, A. Passarelli, M. I. Ferrante, M. R. d'Alcalà, and M. Montresor. 2020. Density-dependent mechanisms regulate spore formation in the diatom *Chaetoceros socialis*. Limnol. Oceanogr.: Lett. **5**: 371–378. doi:10.1002/lol2.10159

Rembauville, M., S. Blain, L. Armand, B. Quéguiner, and I. Salter. 2015. Export fluxes in a naturally iron-fertilized area of the Southern Ocean – Part 2: Importance of diatom resting spores and faecal pellets for export. Biogeosciences **12**: 3171–3195. doi:10.5194/bg-12-3171-2015

Rynearson, T. A., K. Richardson, R. S. Lampitt, M. E. Sieracki, A. J. Poulton, M. M. Lyngsgaard, and M. J. Perry. 2013. Major contribution of diatom resting spores to vertical flux in the sub-polar North Atlantic. Deep Sea Res. Part I Oceanogr. Res. Pap. **82**: 60–71. doi:10.1016/j.dsr.2013.07.013

Shimizu, K., Y. Del Amo, M. A. Brzezinski, G. D. Stucky, and D. E. Morse. 2001. A novel fluorescent silica tracer for biological silicification studies. Chem. Biol. **8**: 1051–1060. doi:10.1016/S1074-5521(01)00072-2

Shipe, R. F., M. A. Brzezinski, C. Pilskaln, and T. A. Villareal. 1999. Rhizosolenia mats: An overlooked source of silica production in the open sea. Limnol. Oceanogr. **44**: 1282–1292. doi:10.4319/lo.1999.44.5.1282

Sjöqvist, C. O., and A. Kremp. 2016. Genetic diversity affects ecological performance and stress response of marine diatom populations. ISME J. **10**: 2755–2766. doi:10.1038/ismej.2016.44

Tréguer, P., C. Bowler, B. Moriceau, and others. 2018. Influence of diatom diversity on the ocean biological carbon pump. Nat. Geosci. **11**: 27–37. doi:10.1038/s41561-017-0028-x

Utermöhl, H. 1958. Zur Vervollkommnung der quantitativen Phytoplankton-Methodik. Int. Vereinigung für Theor. und Angew. Limnol. Mitteilungen **9**: 1–38. doi:10.1080/05384680.1958.11904091

Wolf, K. K. E., C. J. M. Hoppe, and B. Rost. 2018. Resilience by diversity: Large intraspecific differences in climate change responses of an Arctic diatom. Limnol. Oceanogr. **63**: 397–411. doi:10.1002/lno.10639

Wolf, K. K. E., E. Romanelli, B. Rost, U. John, S. Collins, H. Weigand, and C. J. M. Hoppe. 2019. Company matters: The presence of other genotypes alters traits and intraspecific selection in an Arctic diatom under climate change. Glob. Chang. Biol. **25**: 2869–2884. doi:10.1111/gcb.14675

Znachor, P., and J. Nedoma. 2008. Application of the PDMPO technique in studying silica deposition in natural populations of *Fragilaria crotensis* (Bacillariophyceae) at different depths in a eutrophic reservoir. J. Phycol. **44**: 518–525. doi:10.1111/j.1529-8817.2008.00470.x

Conflict of Interest

None declared.